

Coexistence of electron and hole transport in graphene

S. Wiedmann,¹ H. J. van Elferen,¹ E. V. Kurganova,¹ M. I. Katsnelson,² A. J. M. Giesbers,³
A. Veligura,⁴ B. J. van Wees,⁴ R. V. Gorbachev,⁵ K. S. Novoselov,⁵ J. C. Maan,¹ and U. Zeitler¹

¹*Radboud University Nijmegen, Institute for Molecules and Materials and High Field Magnet Laboratory,
Toernooiveld 7, 6525 ED Nijmegen, The Netherlands*

²*Radboud University Nijmegen, Institute for Molecules and Materials,
Heyendaalseweg 135, 6525 AJ Nijmegen, The Netherlands*

³*Max-Planck-Institut für Festkörperforschung, Heisenbergstraße 1, 70569 Stuttgart, Germany*

⁴*Physics of Nanodevices, Zernike Institute for Advanced Materials,
University of Groningen, Nijenborgh 4, 9747 AG Groningen, The Netherlands*

⁵*Department of Physics, University of Manchester, M13 9PL Manchester, United Kingdom*

(Dated: December 1, 2018)

When sweeping the carrier concentration in monolayer graphene through the charge neutrality point, the experimentally measured Hall resistivity shows a smooth zero crossing. Using a two-component model of coexisting electrons and holes around the charge neutrality point, we unambiguously show that both types of carriers are simultaneously present. For high magnetic fields up to 30 T the electron and hole concentrations at the charge neutrality point increase with the degeneracy of the zero-energy Landau level, which implies a quantum Hall metal state at $\nu=0$ made up by both electrons and holes.

PACS numbers: 73.43.-f, 73.63.-b, 71.70.Di

1. INTRODUCTION

The carrier concentration in semiconductors is commonly measured using the Hall effect based on the Lorentz force exerted on moving charged particles in a perpendicular magnetic field [1]. In conventional finite-gap semiconductors, the low-temperature Hall resistivity ρ_{xy} directly measures either the electron or the hole density. However, in compensated semiconductors, where electrons and holes coexist, the Hall resistivity is determined by *both* types of carriers and, in particular, becomes zero in a fully compensated material.

Graphene is an ideal two-dimensional zero-gap semiconductor with a linear dispersion [2] where the electron and hole concentration at $T=0$ go to zero when sweeping the carrier density through the charge neutrality point (CNP). However, non-perfect samples with random potential fluctuations will break up into spatially inhomogeneous conducting electron-hole puddles [3] leaving a finite number of electrons and holes directly at the CNP.

In this article, we present experimental results on the Hall resistivity ρ_{xy} in graphene around the CNP in magnetic fields up to 30 T and for temperatures down to 0.5 K. We demonstrate that the smooth zero-crossing of ρ_{xy} at the CNP for all magnetic fields is caused by a finite concentration of both electrons and holes below and above the CNP with an equal number of electron and hole states occupied at the CNP. We show that the measured carrier concentration increases linearly with the magnetic field which is related to the degeneracy of the zero-energy LL shared equally between electrons and holes.

We have investigated three different graphene devices made from Kish graphite (sample A) and natural graphite (samples B and C) with mobilities between $\mu = 0.8 \text{ m}^2\text{V}^{-1}\text{s}^{-1}$ for sample A and $\mu = 1 \text{ m}^2\text{V}^{-1}\text{s}^{-1}$

for samples B and C. Single-layer graphene flakes were deposited on a Si/SiO₂ substrate, identified optically [4] and patterned using standard techniques [2, 5]. The total charge-carrier concentration q in the graphene films, defined as $q \equiv n - p \simeq \alpha V_g$, can be adjusted from hole-doped ($q < 0$) to electron doped ($q > 0$) by means of a back-gate voltage V_g . Here n and p are the carrier concentrations for electrons and holes, respectively, and $\alpha = 7.2 \times 10^{14} \text{ m}^{-2} \text{ V}^{-1}$ for a 300-nm thick SiO₂ gate insulator. In order to remove surface impurities, all devices were annealed at 440 K prior to the low-temperature measurements. Admixtures of ρ_{xx} to ρ_{xy} due to contact misalignment and inhomogeneities we removed by symmetrization of all traces measured in positive and negative magnetic fields.

The paper is organized as follows: Section II presents our experimental results. The first part of Section II shows transport measurements at low magnetic fields where the Hall resistance is not yet quantized and charge carriers can be considered as “free” (mobile). The second part presents data up to 30 T in the quantum Hall (QH) regime. Section III develops a model for the density of states in graphene, first applied to our samples and then we discuss different splitting scenarios of the lowest Landau level. Concluding remarks are given in the last section.

2. EXPERIMENTAL RESULTS

We first present measurements of Hall resistivity ρ_{xy} with increasing magnetic field in Fig. 1(a) for sample A as a function of total carrier concentration q for several magnetic fields at $T=1.3 \text{ K}$. The corresponding back-gate voltage V_g is displayed on the top-axis. For $B=15 \text{ T}$,

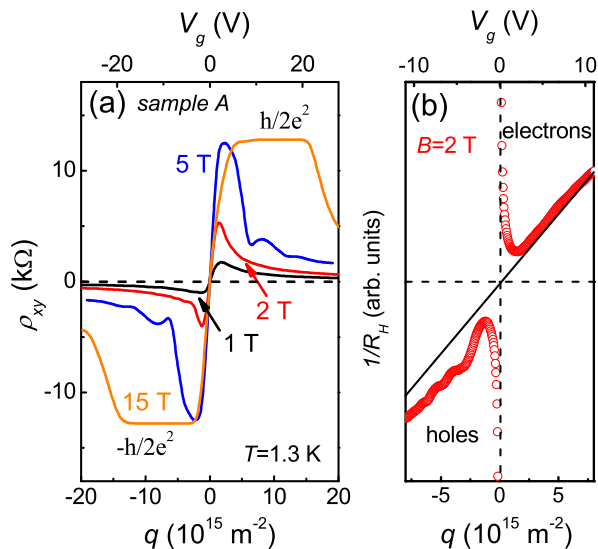


FIG. 1: (Color online) (a) Dependence of ρ_{xy} in sample A on the carrier concentration (bottom axis) or on the back-gate voltage V_g (top axis) for several magnetic fields at $T=1.3$ K. (b) Inverse Hall coefficient $1/R_H$ as a function of q for $B=2$ T. The solid line shows the expected behavior of a conventional zero-gap semiconductor where electrons and holes get fully depleted at the CNP.

ρ_{xy} exhibits Hall plateaus quantized to $\rho_{xy} = \pm h/2e^2$ at filling factors $\nu = \pm 2$. For all magnetic fields, the Hall resistance is not diverging at the CNP when either electron or hole states are depleted. ρ_{xy} rather moves smoothly through zero from the $\nu = -2$ plateau to the $\nu = +2$ plateau.

In order to accommodate for this simple experimental observation, we describe the inverse Hall coefficient $1/R_H = B/\rho_{xy}$ with a two-carrier model for electrons and holes as known for compensated semiconductors [6]

$$\frac{1}{R_H} = \frac{e(n\mu_n + p\mu_p)^2}{n\mu_n^2 - p\mu_p^2}. \quad (1)$$

n and p are the electron and hole concentrations and μ_e and μ_h are the electron and hole mobilities, respectively. In our graphene samples the measured conductivity as a function of carrier concentration is symmetric around the CNP and we can therefore assume the same mobility for both electrons and holes, $\mu_n = \mu_p$, and Eq. (1) simplifies to

$$\frac{1}{R_H} = \frac{e(n+p)^2}{(n-p)}. \quad (2)$$

It is worth emphasizing that we can apply the two-carrier model despite the presence of electron-hole puddles, which would result, for conventional nonrelativistic charge carriers, in spatial separation and related percolation phenomena in electron and hole regions. In the

two-dimensional case, the percolation over electron puddles blocks unavoidably the transport for holes, and vice versa. The case of graphene is dramatically different. The crucial point is that for graphene the borders between p and n regions are actually transparent, and electrons and holes transfer smoothly into each other, which is referred to as Klein tunneling [7]. At specific magic angles of incidence (including normal incidence) the transmission probability is 100%. The presence of a magnetic field does not destroy the Klein tunneling but just shifts the magic angles [8]. It can be assumed that tunneling from one electron puddle to the other electron puddle always remains possible even for carriers incident to an oblique angle (the same holds for hole transport). Thus, even under a nonuniform distribution of electron-hole puddles, we can apply our two-carrier model to graphene.

Fig. 1(b) shows the inverse Hall coefficient $1/R_H$ as a function of q for $B=2$ T extracted from our measurements. For high q , $1/R_H$ exhibits a linear increase due to the presence of either electrons ($q > 0$) or holes ($q < 0$). For $q \rightarrow 0$, however, the simultaneous presence of two distinct types of charge carriers around the CNP immediately becomes visible as a divergence of $1/R_H$ around the CNP, which in turn implies that $n + p$ must remain finite.

2.1. Low magnetic fields

We now present low-field data in Fig. 2 for sample B measured at 0.5 K and in magnetic fields where the quantum Hall effect (QHE) is not yet developed. Using Eq. (2) we extract the individual charge-carrier concentrations n and p as a function of the total charge density q [see Fig. 2(b)]. Both charge carriers are present above and below the CNP and the electron (hole) concentration already starts to increase as the hole (electron) concentration is still decreasing. Precisely at the CNP, we extract a charge-carrier concentration $n(q=0) = p(q=0) = 4.2 \times 10^{14} \text{ m}^{-2}$ only weakly dependent on B for $0 < B < 4$ T. Away from the CNP, the system remains two-component and the minority charge carriers only disappear for $|q| > 2 \times 10^{15} \text{ m}^{-2}$. The same analysis for the other two samples qualitatively yields similar results with $n(q=0) = p(q=0) = 7.4 \times 10^{14} \text{ m}^{-2}$ for sample A and $n(q=0) = p(q=0) \simeq 5 \cdot 10^{14} \text{ m}^{-2}$ for sample C. The fact that the sample with the lowest mobility (sample A) reveals the highest $n(q=0)$ qualitatively confirms a scenario of coexisting electron-hole puddles, where lower mobilities are generally associated with larger potential fluctuations.

2.2. Quantum Hall regime

We now turn our attention to measurements in high magnetic fields. We present experimental data from 5 to 25 T both for longitudinal resistivity ρ_{xx} and Hall

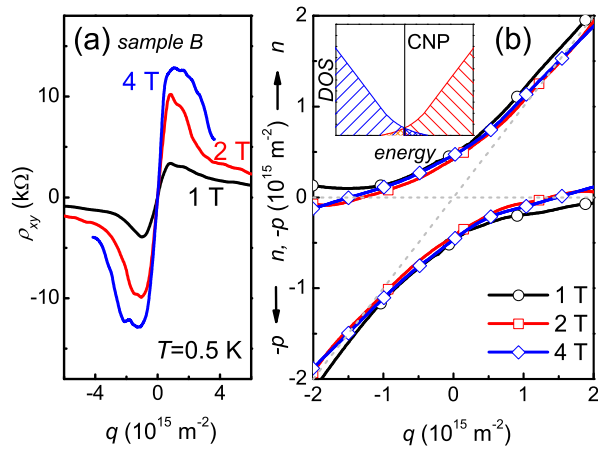


FIG. 2: (Color online) (a) Low-field Hall resistivity ρ_{xy} and (b) extracted carrier concentration for electrons n and holes p as a function of total charge q according to Eq. (2) for sample B. Both types of charge carriers are present for $|q| < 2 \cdot 10^{15} \text{ m}^{-2}$. Inset: Sketch of the DOS for $B=0$ at the CNP.

resistivity ρ_{xy} [see Fig. 3(a) and Fig. 3(b)] measured in sample C at $T=4 \text{ K}$. ρ_{xy} is measured from $B=5 \text{ T}$ up to 25 T in steps of 5 T . ρ_{xy} is now quantized at $\nu = \pm 2$ but still shows a smooth zero-crossing from $\rho_{xy} = -h/2e^2$ to $\rho_{xy} = +h/2e^2$ without any sign of divergence at the CNP. Consequently, we still find a finite charge carrier concentration for electrons and holes around the CNP as depicted in Fig. 3(c). Therefore, we can conclude that electrons still contribute to conduction below $E=0$ and holes do so above $E=0$. It should be noticed that in the range of magnetic fields used for the extraction of the carrier densities, ρ_{xx} does not affect ρ_{xy} even if we take into account a small amount of mixing between both signals but becomes relevant if ρ_{xx} starts diverging at the CNP.

In addition, we now observe an increase of n and p with increasing magnetic field. This field-dependent carrier concentration around the CNP is elucidated further in Fig. 4 where we plot the electron concentration at the CNP as a function of magnetic field for all investigated samples. For low magnetic fields ($B < 5 \text{ T}$), $n(q=0)$ remains constant and can be explained by the presence of electron-hole puddles.

For higher magnetic fields, $n(q=0)$ starts to increase linearly with B reflecting the B -proportional degeneracy n_L for each of the four sub-levels in the zero-energy Landau level (LL) [9, 10]. Since, at the CNP, half of the possible electrons states and half of the hole states are filled, respectively, we expect n_L electron states and n_L hole states occupied per unit area. Therefore, for comparison, we have also plotted n_L in Fig. 4. Interestingly, we only observe about 30 % of the expected electron and hole concentration n_L in our data extracted from the Hall experiments.

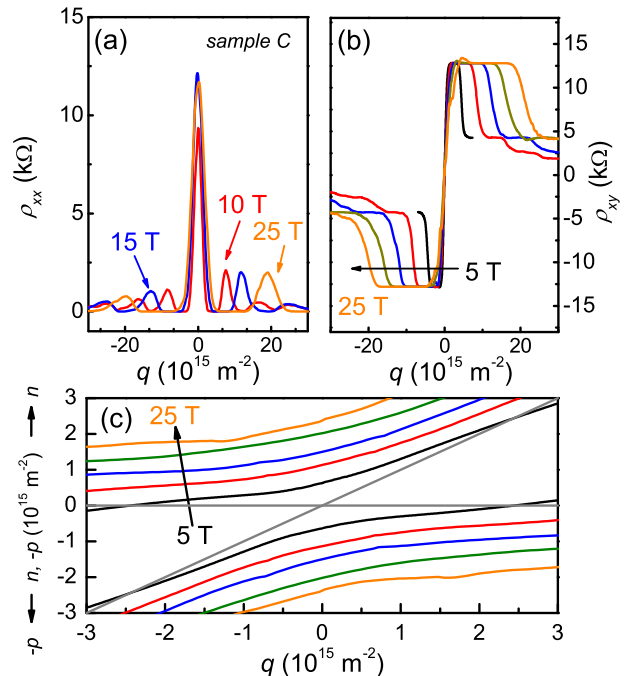


FIG. 3: (Color online) (a) High-field Hall resistivity ρ_{xy} and longitudinal resistivity ρ_{xx} of sample C at 4 K for different magnetic fields. (c) Corresponding charge-carrier concentrations n and p extracted according to Eq. (2).

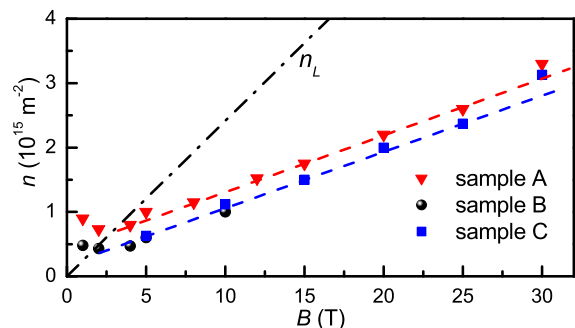


FIG. 4: (Color online) Charge-carrier concentration at the CNP as a function of magnetic field for all samples (the dashed-dotted line depicts degeneracy n_L).

In contrast to low magnetic fields, where the QHE is not yet developed and all charge carriers can be considered as mobile, we now have to take into account localized charge carriers in the tails of the LLs in the quantized regime. This fact is essentially reflected in Fig. 4, where we extracted the density for electrons and holes using Eq. (2) from the Hall resistivity, which only takes free charge carriers into account. To further support our

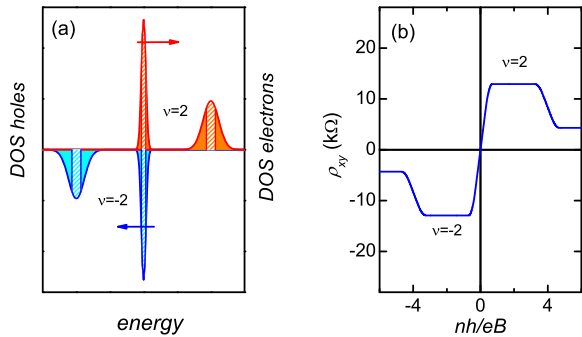


FIG. 5: (Color online) (a) Four-fold degenerate zeroth LL with coexisting electrons and holes below and above the CNP (the electron levels (red) are sketched upward and the hole levels (blue) are sketched downward). (b) Smooth zero-crossing of the Hall resistance from $\nu=-2$ to $\nu=2$.

assumption that about 30 % of the charge carriers are indeed free, we take a look at the broadening of LLs and the ratio between extended and localized states depending on the strength of the magnetic field which has been extracted from temperature-dependent measurements [11] and QH plateaus at high B . Indeed, we observe a good agreement with our findings that only 30 % of the total carrier concentration is measured as free charge carriers.

3. DENSITY OF STATES MODEL

3.1. Investigated samples

The above measurements allow us to sketch the density of states (DOS) for electrons and holes. For $B=0$ (see inset to Fig. 2) the DOS in graphene $D(E) = 2|E|/\pi(\hbar v)^2$ (v is the Fermi velocity) is smeared out around the CNP due to the presence of electron-hole puddles. Applying a magnetic field leads to a quantization of the DOS, shown in Fig. 5(a). Electrons and holes in the center of the LLs are extended (shaded areas) whereas they are localized in the Landau level tails (filled areas). In that picture the LLs $N=0$ and $N=1$ are well separated, yielding quantized plateaus in ρ_{xy} at $\nu = \pm 2$ [Fig. 3(a)] when the Fermi energy is situated in the localized tails of the LLs.

Within this DOS model (see also Ref. [12]) we can now calculate the longitudinal conductivity σ_{xx} by means of the Kubo-Greenwood formalism [13, 14] and the Hall conductivity σ_{xy} summing up all states below the Fermi energy [15]. Including the presence of electrons and holes above and below the CNP indeed yields a smooth zero crossing of ρ_{xy} as measured in Fig. 3(a) and modeled in Fig. 5(b).

Our experimental observation of coexisting electrons and holes around the CNP also has a direct implication

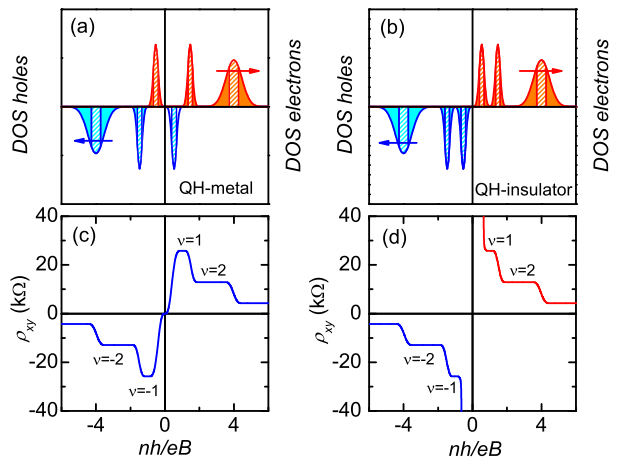


FIG. 6: (Color online) Sketched DOS for (a) a QH-metal and (b) a QH-insulator if both spin and valley splitting is resolved. (c) Smooth zero-crossing of the Hall resistivity if both charge carriers are present above and below the CNP and (d) diverging ρ_{xy} due to electrons and holes being separated and residing on different sides of the CNP.

on the nature of the $\nu=0$ QHE in graphene [16]. Neither a gap opening at the CNP [12], nor a complete lifting of spin and valley degeneracy, if we assume the spin first scenario of the zeroth LL [17], fundamentally change the zero-crossing of the Hall resistance. Our experimental results up to a magnetic field of 30 T do not exhibit interaction-driven QHE [18] due to a larger disorder confirmed by lower mobility in our samples compared to Ref. [17]. If we calculate σ_{xy} and σ_{xx} from measured ρ_{xy} and ρ_{xx} using standard matrix inversion our samples show the gap opening in σ_{xx} at $B=30$ T due to increasing ρ_{xx} at the CNP. Consequently, a small plateau in σ_{xy} at the CNP appears whereas the Hall resistance smoothly crosses through zero [12].

3.2. Splitting scenarios of the lowest Landau level

In samples with lower disorder, spin and valley degeneracies are lifted. As demonstrated in Ref. [17], the Hall resistivity exhibits a smooth zero-crossing (with fluctuations) from the $\nu=-1$ plateau to the $\nu=1$ plateau with increasing V_g . We have calculated the DOS assuming that both electrons and holes exist above and below the CNP [Fig. 6(c)] and find the smooth zero-crossing of the Hall resistivity [see Fig. 6(c)].

Furthermore, we use our DOS model to directly address the question whether $\nu=0$ is a QH-metal or a QH-insulator. Measurements of longitudinal resistance have shown either finite ρ_{xx} , even subjected to high magnetic fields (QH-metal) [9, 10, 17, 19] or a steeply increase in

ρ_{xx} , attributed to an insulating ground state [20]. The first observation is generally explained by an insulating bulk and conducting channels at the sample edges [19]. Both scenarios are directly related to the lifting of degeneracy of the zeroth LL. Whereas in a QH-metal spin splitting is larger than valley splitting, in a QH-insulator the contrary is the case. If spin and valley degeneracy is lifted, a zero-crossing of ρ_{xy} is observed if we include the presence of electrons and holes above and below the CNP, see Fig. 6(a) and (c). However, if we separate electrons and holes at the CNP, see Fig. 6(b) (valley first scenario), ρ_{xy} diverges (see Fig. 6(d)). The divergence of ρ_{xy} in the valley first scenario beyond filling factor $\nu=1$ when approaching the CNP has indeed been recently found in high mobility graphene devices, fabricated on a single-crystal boron nitride substrate [21] and thus confirm our DOS model. However, beyond fractional filling factor $\nu=1/3$, ρ_{xy} starts to decrease strongly and might pass through zero. This behavior would imply positive and negative charged composite fermions around the CNP.

4. CONCLUSION

In conclusion, we have performed measurements of the Hall resistivity in graphene in a magnetic field up to 30 T.

ρ_{xy} does not diverge at the CNP but shows a smooth transition from electrons to holes. Our analysis based on mixed conduction at the CNP implies that both electrons and holes exist both below and above the CNP with as many hole states as electron states occupied at the CNP. Charge-carrier concentration as a function of magnetic field is explained as a transition from transport dominated by electron-hole puddles to a quantized DOS with increasing B . Taking into account the presence of both charge carriers above and below the CNP contributes to a better understanding of the unique nature of electronic states at the lowest LL in graphene.

Finally, we have to point out that physics around the CNP, such as the behavior of ρ_{xy} from hole-dominated to electron-dominated transport becomes easier to access with high-mobility samples even though diverging ρ_{xx} directly affects the extraction of Hall resistivity under realistic experimental conditions.

Part of this work has been supported by EuroMagNET II under the EU contract number 228043 and by the Stichting Fundamenteel Onderzoek der Materie (FOM) with financial support from the Nederlandse Organisatie voor Wetenschappelijk Onderzoek (NWO).

-
- [1] E. H. Hall, American Journal of Mathematics vol **2**, 287 (1879).
 - [2] A. K. Geim and K. S. Novoselov, Nat. Mater. **6**, 183 (2007).
 - [3] J. Martin, N. Akerman, G. Ulbricht, T. Lohmann, J. H. Smet, K. von Klitzing, A. Yacobi, Nat. Phys. **4**, 144 (2008).
 - [4] P. Blake, E. W. Hill, A. H. Castro Neto, K. S. Novoselov, D. Jiang, R. Yang, T. J. Booth, and A. K. Geim, Appl. Phys. Lett. **91**, 063124 (2007).
 - [5] K. S. Novoselov, A. K. Geim, S. V. Morozov, D. Jiang, Y. Zhang, S. V. Dubonos, I. V. Grigorieva, and A. A. Firsov, Science **306**, 666 (2004).
 - [6] see, e.g., K. Seeger, *Semiconductor physics, an introduction*, 5th ed., p. 61, Springer, Berlin (1997).
 - [7] M. I. Katsnelson, K. S. Novoselov, and A. K. Geim, Nature Phys. **2**, 620 (2006).
 - [8] A. F. Young and P. Kim, Nature Phys. **5**, 222 (2009).
 - [9] K. S. Novoselov, A. K. Geim, S. V. Morozov, D. Jiang, M. I. Katsnelson, I. V. Grigorieva, S. V. Dubonos, and A. A. Firsov, Nature (London) **438**, 197 (2005).
 - [10] Y. Zhang, Y. Tan, H. L. Stormer, and P. Kim, Nature (London) **438**, 201 (2005).
 - [11] A. J. M. Giesbers, U. Zeitler, M. I. Katsnelson, L. A. Ponomarenko, T. M. Mohiuddin, and J. C. Maan, Phys. Rev. Lett. **99**, 206803 (2007).
 - [12] A. J. M. Giesbers, L. A. Ponomarenko, K. S. Novoselov, A. K. Geim, M. I. Katsnelson, J. C. Maan, and U. Zeitler, Phys. Rev. B **80**, 201403(R) (2009).
 - [13] R. Kubo, Canad. J. Phys. **34**, 1274-1277 (1956).
 - [14] D. A. Greenwood, Proc. Phys. Soc. London **71**, 585-596 (1958).
 - [15] P. Streda, J. Phys. C: Solid. State Phys. **15**, 717-721 (1982).
 - [16] S. Das Sarma and K. Yang, Solid State Commun. **149**, 1502 (2009).
 - [17] Y. Zhang, Z. Jiang, J. P. Small, M. S. Purewal, Y. W. Tan, M. Fazlollahi, J. D. Chudow, J. A. Jaszczak, H. L. Stormer, and P. Kim, Phys. Rev. Lett. **96**, 136806 (2006).
 - [18] K. Nomura and A. H. MacDonald, Phys. Rev. Lett. **96**, 256602 (2006).
 - [19] D. A. Abanin, K. S. Novoselov, U. Zeitler, P. A. Lee, A. K. Geim, and L. S. Levitov, Phys. Rev. Lett. **98**, 196806 (2007).
 - [20] J. G. Checkelsky, L. Li, and N. P. Ong, Phys. Rev. Lett. **100**, 206801 (2008); Phys. Rev. B **79**, 115434 (2009).
 - [21] C. R. Dean, A. F. Young, P. Cadden-Zimansky, L. Wang, H. Ren, K. Watanabe, T. Taniguchi, P. Kim, J. Hone, K. L. Shepard, Nature Phys., **5**, 693 (2011).